Self-sustained Maser oscillations of a large magnetization driven by a radiation damping-based electronic feedback

Daniel Abergel, Alain Louis-Joseph, Jean-Yves Lallemand

Self-sustained Maser oscillations of a large magnetization driven by a radiation damping-based electronic feedback

Daniel Abergel, Alain Louis-Joseph, and Jean-Yves Lallemand

Articles you may be interested in

Experimental evaluation of anti-sound approach in damping self-sustained thermoacoustics oscillations
J. Appl. Phys. **114**, 204903 (2013); 10.1063/1.4833238

Free-electron maser based on a cavity with two- and one-dimensional distributed feedback
Appl. Phys. Lett. **92**, 211501 (2008); 10.1063/1.2924313

Theory of free-electron maser with two-dimensional distributed feedback driven by an annular electron beam
J. Appl. Phys. **92**, 1619 (2002); 10.1063/1.1481193

Dynamical instabilities in liquid nuclear magnetic resonance experiments with large nuclear magnetization, with and without pulsed field gradients
J. Chem. Phys. **116**, 8439 (2002); 10.1063/1.1469020

Nuclear magnetic resonance spin echoes for restricted diffusion in an inhomogeneous field: Methods and asymptotic regimes
J. Chem. Phys. **114**, 6878 (2001); 10.1063/1.1356010

Self-sustained Maser oscillations of a large magnetization driven by a radiation damping-based electronic feedback

Daniel Abergel,[a] Alain Louis-Joseph, and Jean-Yves Lallemand
Laboratoire DCSO-Groupe de RMN Ecole Polytechnique 91128 Palaiseau Cedex, France

In this paper, the dynamics of a magnetization undergoing a radiation-damping based feedback radio-frequency field is investigated both theoretically and experimentally. It is shown that due to the presence of T_1 relaxation the evolution equations predict the existence of self-sustained maser pulses. This phenomenon is a consequence of the competition between two different processes, namely, T_1 relaxation and a precession about a magnetization-dependent radio-frequency field. Experiments show the existence of periodic revivals of the free induction decay over unusually long periods of time, on the order of tens of seconds. © *2002 American Institute of Physics.*
[DOI: 10.1063/1.1462583]

I. INTRODUCTION

The dynamics of an ensemble of spins that do not exhibit mutual coupling is usually well described by the Bloch equations. It can be viewed as the combination of a precession about a (possibly time-dependent) magnetic field and of a relaxation process, which gives rise to a damping of the transverse component of the magnetization with the relaxation time constant T_2, whereas the longitudinal component returns to equilibrium with the time constant T_1. In certain situations, however, this description fails despite the absence of direct short range spin–spin interactions that would involve a more complex description using the density matrix formalism. In this respect, the presence of radiation damping is particularly interesting. In that case, although the spin ensemble may still be described by a classical magnetization vector, the Bloch equations need be modified in such a way that the evolution of the magnetization is governed by a nonlinear set of differential equations. This is related to the fact that radiation damping results from the interaction of a large precessing magnetization with the radio-frequency field induced by the latter in the detecting coil[1,2] and which depends explicitly on the magnetization components. Radiation damping is important for the conditions typically encountered in high field nuclear magnetic resonance (NMR) experiments and can seriously perturb experiments so that various approaches have been used to eliminate it.[3–6] It is noteworthy that the dynamics of the magnetization induced by radiation damping is usually quite simple. Indeed, for practical purposes it may be simply considered as a precession about a magnetization-dependent radio-frequency field which is perpendicular to the transverse component of the magnetization and forces the magnetization vector back to its equilibrium direction. Recently, the possibility of generating radiation-damping-based radio-frequency feedback fields,

the intensity and phase of which are controlled with respect to the solvent magnetization, was demonstrated[5] in a successful attempt to completely manipulate the solvent magnetization in high-resolution NMR experiments. This approach lead to the concept of ''slaved pulses,'' which are self-calibrated pulses allowing selective rotation of a large magnetization towards the $\pm z$-axis[7] or the *xy*-plane,[8] regardless of its initial direction in space. The ideas underlying such an approach are based on the intuitive model of a feedback field acting on a magnetization in the absence of relaxation. These studies and basically the very possibility of generating a radiation damping based radio-frequency field with arbitrary gain and phase have motivated a detailed study of the resulting dynamics. When transverse T_2 relaxation only is considered, as in Ref. 9, the magnetization dynamics is only slightly affected and the main qualitative features remain unchanged. However, when T_1 relaxation is taken into account, the dynamics may be fairly more complicated and somewhat less intuitive. A closer look at these nonlinear Bloch equations (NLBE) may reveal unexpected features in this case.

In this article we investigate both theoretically and experimentally the dynamics of a magnetization driven by a feedback field with arbitrary values of gain and phase. It will be shown that the latter field may induce unconventional long-time behavior, in the form of repeated bursts of in-plane magnetization, which we call self-sustained maser pulses by analogy with the so called maser pulse caused by radiation damping. In Sec. II the relevant dynamical equations are reviewed and exact solution is given for the case $T_1 = \infty$. In Sec. III a qualitative analysis of the complete differential system ($T_1 < \infty$) is given and asymptotic evolution is studied in this case. In Sec. IV the transient behavior is investigated by numerical simulations. Theoretical predictions will be tested experimentally and the results discussed in Sec. V.

II. THE DYNAMICAL EQUATIONS

Introduction of an externally generated feedback field was first proposed by Kayser some decades ago[10] in the context of CW NMR spectroscopy, where the effect on the line

---

[a]Author to whom correspondence should be addressed. Tel: (+33)1 44 32 33 44; electronic mail: Daniel.Abergel@ens.fr; Permanent address: Laboratoire de Chimie, Ecole Normale Supérieure, 24, rue Lhomond 75005 Paris, France.

shape was emphasized. In the present work, we adopt a dynamical system viewpoint and focus on the time evolution of the magnetization undergoing such a feedback field. Consider a magnetization acted upon by the combined action of a magnetic field $\mathbf{B}_0$ and of an applied radiofrequency field $\mathbf{B}_1$. Its dynamics consists in a precession about the resultant of both fields and a damping of the magnetization components, as described by the Bloch equations. In addition, the intensity of a back action field resulting from magnetization–coil interaction is proportional to the magnitude of the transverse magnetization and its direction in the xy-plane is determined by a constant dephasing ψ with respect to the former. It can be expressed as

$$\mathbf{B}_{\mathrm{FB}} = \gamma G \mathbf{M}_t e^{-i\psi}, \tag{1}$$

where

$$\mathbf{M}_t = M_x + i M_y, \tag{2}$$

G is the enhancement factor (gain) with respect to the magnitude of the transverse magnetization, and ψ is the phase of the feedback field. With these notations, the radiation damping case corresponds to

$$\psi = -\pi/2$$

and

$$G = \frac{\mu_0}{2}\eta Q$$

in SI units.

The dynamical equations governing the evolution of the magnetization in the rotating frame are

$$\begin{cases} \dot{M}_x = \delta M_y + \gamma G M_z (M_x \sin\psi - M_y \cos\psi) - M_x/T_2, \\ \dot{M}_y = -\delta M_x - \omega_1 M_z + \gamma G M_z(M_x \cos\psi + M_y \sin\psi) \\ \qquad - M_y/T_2, \\ \dot{M}_z = \omega_1 M_y - \gamma G \sin\psi(M_x^2 + M_y^2) - (M_z - M_0)/T_1, \end{cases} \tag{3}$$

where $T_{1,2}$ are the longitudinal and transverse relaxation times, respectively. δ is the frequency shift offset. The constant radio-frequency field with intensity $B_1 = \omega_1/\gamma$ was assumed to be aligned along the x-axis in the rotating frame without loss of generality. It is convenient to recast Eqs. (3) by introducing the reduced dimensionless variables, $t \rightarrow \omega_1 t$, $\gamma G \rightarrow \gamma G M_0/\omega_1 = \lambda$, $\delta \rightarrow \delta/\omega_1$, $T_{1,2} \rightarrow \omega_1 T_{1,2}$, and $\mathbf{M} \rightarrow \mathbf{M}/M_0 = \mathbf{m}$. One thus gets

$$\begin{cases} \dot{m}_x = \delta m_y + \lambda m_z(m_x \sin\psi - m_y \cos\psi) - m_x/\tau_2, \\ \dot{m}_y = -\delta m_x - m_z + \lambda m_z(m_y \sin\psi + m_x \cos\psi) \\ \qquad - m_y/\tau_2, \\ \dot{m}_z = m_y - \lambda \sin\psi(m_x^2 + m_y^2) - (m_z - 1)/\tau_1. \end{cases} \tag{4}$$

When relaxation is neglected, the magnetization vector lies on a sphere and the motion is therefore two dimensional. In the case of radiation damping, Eqs. (4) have explicit solutions when $\tau_{1,2} = \infty$.[11] However, as will be seen shortly, when

relaxation is included in the treatment of a back action field, the magnetization dynamics exhibits unusual features and may be more difficult to grasp.

In the remainder of this paper, we will limit the study to the case where no applied $\mathbf{B}_1$ radiofrequency field is present, so that Eqs. (4) write

$$\begin{cases} \dot{m}_x = \delta m_y + \lambda m_z(m_x \sin\psi - m_y \cos\psi) - m_x/\tau_2, \\ \dot{m}_y = -\delta m_x + \lambda m_z(m_y \sin\psi + m_x \cos\psi) - m_y/\tau_2, \\ \dot{m}_z = -\lambda \sin\psi(m_x^2 + m_y^2) - (m_z - 1)/\tau_1. \end{cases} \tag{5}$$

At this point, it is convenient to introduce a new set of variables (u, m_z, ϕ), so that the equations of motion take the following form:

$$\begin{cases} \dot{u}(t) = 2(\lambda m_z \sin\psi - \gamma 2)u, \\ \dot{m}_z(t) = -\lambda \sin\psi u - \gamma_1(m_z - 1), \\ \dot{\phi}(t) = -\delta + \lambda \cos\psi m_z, \end{cases} \tag{6}$$

where

$$u = m_x^2 + m_y^2, \tag{7}$$

$$m_t = m_x + i m_y = \sqrt{u}\, e^{i\phi(t)}, \tag{8}$$

and

$$\gamma_{1,2} = 1/\tau_{1,2}. \tag{9}$$

In this set of equations, the first two are coupled whilst the third one relates the phase of the magnetization to its longitudinal component. Interestingly enough, the precession frequency of the magnetization, given by the third equation of (6), is modulated by the z component of $\mathbf{m}$ so it turns out that during a typical trajectory of the magnetization from $-z$ to $+z$, the former is in general time-dependent. In this respect, radiation damping is a remarkable exception, since one has $\cos\psi = 0$ and the precession frequency is therefore constant with time.

This differential system cannot be solved analytically in the general case. If, however longitudinal T_1 relaxation may be neglected ($\gamma_1 = 0$), then the resulting system

$$\begin{cases} \dot{u}(t) = 2(\lambda m_z \sin\psi - \gamma_2)u, \\ \dot{m}_z(t) = -\lambda \sin\psi u, \end{cases} \tag{10}$$

admits the following solution:

$$\begin{cases} m_z(t) = -C_0(\lambda \sin\psi)^{-1} \tanh(C_0 t + B_0) + \dfrac{\gamma_2}{\lambda \sin\psi}, \\ u = -(\lambda \sin\psi)^{-1} \dot{m}_z(t), \end{cases} \tag{11}$$

where

$$C_0 = \pm \sqrt{(\lambda \sin \psi m_z(0) - \gamma_2)^2 + (\lambda \sin \psi)^2 u(0)} \qquad (12)$$

and

$$B_0 = \operatorname{atanh}\left(\frac{\lambda \sin \psi m_z(0) - \gamma_2}{C_0}\right). \qquad (13)$$

Direct observation of Eqs. (12) and (13) shows that the sign of C_0 is irrelevant, so one can choose the positive root. This equation is the generalization of the solution derived by Bloom[9] for radiation damping to the case of a feedback field of arbitrary phase and gain. The motion of **m** described by Eq. (13) is a rotation towards the north (resp. south) hemisphere of the Bloch sphere when the sign of $\sin \psi$ is negative (resp. positive). It is noteworthy, as was pointed out in Ref. 9, that the maximum of transverse magnetization does not occur when the magnetization vector passes through the xy-plane, but instead when

$$m_z = \frac{\gamma_2}{\lambda \sin \psi}.$$

Note also that, since $\gamma_1 = 0$, this model does not predict a return of the magnetization to $\mathbf{m}_0$. Nevertheless, the magnetization always ends up aligned with the z axis, as is obvious from Eq. (10), with a magnitude that depends on the relative magnitudes of T_2 and the characteristic time defined by analogy with radiation damping,

$$T_{FB}^{-1} = \gamma G |\sin \psi| M(0), \qquad (14)$$

where $M(0)$ is the magnitude of the magnetization at time $t = 0$.

III. T_1 RELAXATION: ASYMPTOTIC BEHAVIOR

When T_1 relaxation is present, the equations of motion cannot be solved exactly, so that one has to resort to numerical computation to study the time evolution of the magnetization. However, valuable information on the long term dynamics of the magnetization can be obtained by making use of results from the theory of nonlinear dynamical systems (see, for instance, Refs. 12 and 13 for a general introduction). It is possible to make a qualitative analysis of this differential system in order to determine the type of motion in the long time limit by studying the stationary solutions of $u(t)$ and $m_z(t)$. Using the language of dynamical system theory, one thus has to first find the fixed points of this set of differential equations and to analyze their stability, i.e., the behavior of the equations in their vicinity. In our case, the fixed points are easily found to be

$$F_1 = (0,1)$$

and

$$F_2 = \left(u^{st} = -\frac{\gamma_1}{\lambda \sin \psi}[m_z^{st} - 1], \quad m_z^{st} = \frac{\gamma_2}{\lambda \sin \psi}\right). \qquad (15)$$

Following standard procedure,[13] the stability analysis is performed by linearizing the system in their vicinity. In the F_1 fixed point system of coordinates $\{U, Z\}$ is defined by

$$\begin{cases} u = U, \\ m_z = Z + 1, \end{cases} \qquad (16)$$

one has

$$\frac{d}{dt}\begin{pmatrix} U \\ Z \end{pmatrix} = \mathbf{L}_1 \begin{pmatrix} U \\ Z \end{pmatrix} + \begin{pmatrix} 2\lambda \sin \psi ZU \\ 0 \end{pmatrix}, \qquad (17)$$

where

$$\mathbf{L}_1 = \begin{pmatrix} 2(\lambda \sin \psi - \gamma_2) & 0 \\ -\lambda \sin \psi & -\gamma_1 \end{pmatrix}, \qquad (18)$$

so that the linearized dynamics is simply given by

$$\frac{d}{dt}\begin{pmatrix} U \\ Z \end{pmatrix} = \mathbf{L}_1 \begin{pmatrix} U \\ Z \end{pmatrix}. \qquad (19)$$

The eigenvalues of $\mathbf{L}_1$, which determine the local behavior of the differential system, are given by

$$\begin{cases} x_p = 2(\lambda \sin \psi - \gamma_2), \\ x_m = -\gamma_1. \end{cases} \qquad (20)$$

Similarly, in a neighborhood of F_2, with the new set of coordinates,

$$\begin{cases} u = U + u^{st}, \\ m_z = Z + m_z^{st}, \end{cases} \qquad (21)$$

Eq. (6) write

$$\frac{d}{dt}\begin{pmatrix} U \\ Z \end{pmatrix} = \mathbf{L}_2 \begin{pmatrix} U \\ Z \end{pmatrix} + \begin{pmatrix} 2\lambda \sin \psi ZU \\ 0 \end{pmatrix}, \qquad (22)$$

where

$$\mathbf{L}_2 = \begin{pmatrix} 0 & 2\lambda \sin \psi u^{st} \\ -\lambda \sin \psi & -\gamma_1 \end{pmatrix}. \qquad (23)$$

So that the linearized system in the vicinity of F_2 is

$$\frac{d}{dt}\begin{pmatrix} U \\ Z \end{pmatrix} = \mathbf{L}_2 \begin{pmatrix} U \\ Z \end{pmatrix}, \qquad (24)$$

where $\mathbf{L}_2$ has the following eigenvalues:

$$x_\pm = \frac{-\gamma_1 \pm \sqrt{\Delta}}{2}, \qquad (25)$$

with

$$\Delta = \gamma_1(\gamma_1 + 8\gamma_2 - 8\lambda \sin \psi). \qquad (26)$$

A local analysis of the stability of these fixed points will now be performed. The stability of F_1 (F_2, resp.) depends on the sign of the eigenvalues of $\mathbf{L}_1$ ($\mathbf{L}_2$, resp.). Briefly stated, the different possible situations are the following. If at a given fixed point both eigenvalues are strictly negative (have negative real parts, resp.), the fixed point is said to be a stable node (focus, resp.) and is an attractor. If both eigenvalues are strictly positive (have positive real parts, resp.), the fixed point is an unstable node (focus, resp.). Finally, for real eigenvalues of opposite signs, the fixed point is a saddle and should be considered unstable. These various situations are depicted in Fig. 1.

Now, consider the case where $\sin \psi < 0$. From Eqs. (20) and (25), it is clear that F_1 is always stable and that F_2 is a saddle. The consequence is that the system relaxes towards equilibrium. This is in particular the case for radiation damp-
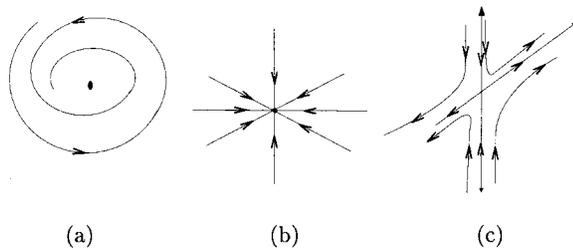
FIG. 1. Schematic representation of the different types of fixed points. Arrows indicate the direction of the flow. (a) Stable node ($\lambda_{1,2} < 0$); (b) stable focus (Re($\lambda_{1,2}$) < 0): the flow spirals inwards towards the fixed point; (c) saddle ($\lambda_{1,2} > 0$): the flow is attracted towards the fixed point along one direction and repelled from it along the other.

ing where $\sin \psi = -1$. For the case $\sin \psi > 0$ it is seen that for $\lambda \sin \psi < \gamma_2$, F_1 is a stable node and it is easily verified that $\Delta > 0$ and F_2 is a saddle, so that the steady state solution at long times is thermal equilibrium. Alternatively, when $\lambda \sin \psi > \gamma_2$, F_1 is a saddle and F_2 is a stable node ($\Delta > 0$) or a stable focus ($\Delta < 0$). Stability diagrams corresponding to the various situations discussed here are shown in Fig. 2.

The interpretation of F_2 being a focus is interesting, since it predicts a damped oscillatory decay of u at long times at the rate $\gamma_1/2$. This means that the magnitude of both the longitudinal and the in-plane magnetization should decay at a rate $1/T_1$ and oscillate at the angular frequency $\sqrt{\Delta}/2$. This is a particularly interesting result, since it actually predicts periodic revivals of the free induction decay, which can be interpreted as repeated self-sustained maser oscillations. Note that the term maser is used here in reference to the fact that radiation damping is the resulting process of an ensemble of spins interacting with the radiofrequency field of a high Q NMR probe and which may radiate spontaneously in a cooperative way. Further, these repetitive maser pulses can indeed be termed self-sustained, because they appear without any radio-frequency excitation other than the feedback field from the probe. It is interesting to remark that although this attractor is a fixed point for (u, m_z), it is not an equilibrium state for the magnetization. Indeed, according to Eq. (6), the motion of the latter in the rotating frame is a precession in a cone defined by

$$\text{atan}(\theta) = -\frac{\gamma_1}{\gamma_2}\left(\frac{\gamma_2}{\lambda \sin \psi} - 1\right) \tag{27}$$
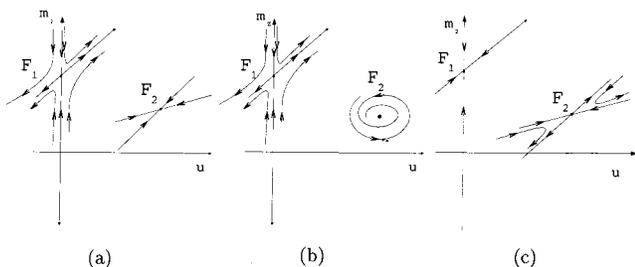
at the rate

FIG. 2. Stability diagrams of the NLBE. In (a), F_1 is a saddle and F_2 is a stable node; (b) F_1 is a saddle and F_2 is a focus; (c) F_1 is a stable node and F_2 is a saddle.

$$\omega(t) = \dot{\phi}(t) = -\delta + \gamma_2 \cot \psi. \tag{28}$$

It is also noteworthy that, in contrast with the case where longitudinal relaxation is absent, the stationary state of the magnetization is not necessarily parallel to the z axis. This is a consequence of the presence of two competing processes, namely, thermal relaxation towards a thermodynamical equilibrium and a back action of the detecting coil on the magnetization which tends to drive the magnetization towards the south pole.[14] Note also that Eqs. (25) and (26) show that the case $\Delta > 0$ involves relatively large relaxation rates compared to $\lambda \sin \psi$, so that the effect of the feedback field upon magnetization is weak and F_2 is located near F_1, close to the z axis.

IV. TRANSIENT BEHAVIOR

The main goal of the previous section was to qualitatively characterize the way the stationary solution of the magnetization is approached at long times. It was shown that the NLBE admits asymptotic solutions with a characteristic evolution time on the order of $1/T_1$ for both the longitudinal and transverse magnetizations, which implies the existence of long lasting transients. In order to complete the study of this simple model and to get a deeper understanding of the spin dynamics described by the NLBE (5), we investigated the transient behavior of this simple model of nonlinear NMR dynamics. Numerical simulations were therefore performed for a feedback field of fixed intensity, while its phase was varied. The magnetization was initially tilted from equilibrium by a small angle ($10^{-2}\pi$) and its evolution numerically computed from Eq. (5). The relaxation parameters used in the simulations were $T_1 = 3$ s and $T_2 = 140$ ms, respectively, and $\delta = -30$ Hz. For the simulations calculated at variable feedback field phase ψ, the gain λ is set to $\lambda = 100$, which would correspond to a radiation damping time of $T_{RD} = 10$ ms (Fig. 3). Alternatively, simulations were also performed with $\psi = \pi/2$ and various values of λ (see Fig. 4). The solutions of the three magnetization components are displayed on the left-hand side of Figs. 3 and 4. On the other hand, the trajectory in the (u, m_z)-space is represented on the right-hand side of Figs. 3 and 4, where the (u, m_z) point spirals inwards towards the fixed point. The most striking feature exhibited by these graphs and which cannot be accounted for by the simpler model where T_1 is absent is the prediction of multiple maserlike pulses during the course of evolution. Indeed one observes revivals of the free induction decay, which occur repeatedly at unusually long time intervals (several seconds).

The existence of such maser pulses depends on three different time constants. The first one is the condition for at least one inversion pulse to occur, that is $T_{FB} < T_2$. The second important time scale is the longitudinal relaxation time T_1, which determines, together with T_2, the possibility of recurrent pulses to take place, as seen from the conditions under which $\Delta < 0$ (26). It is noteworthy that during these bursts of in-plane magnetization, the magnetization vector does not necessarily cross the xy-plane, as seen from the z component of the magnetization depicted in Figs. 3 and 4.
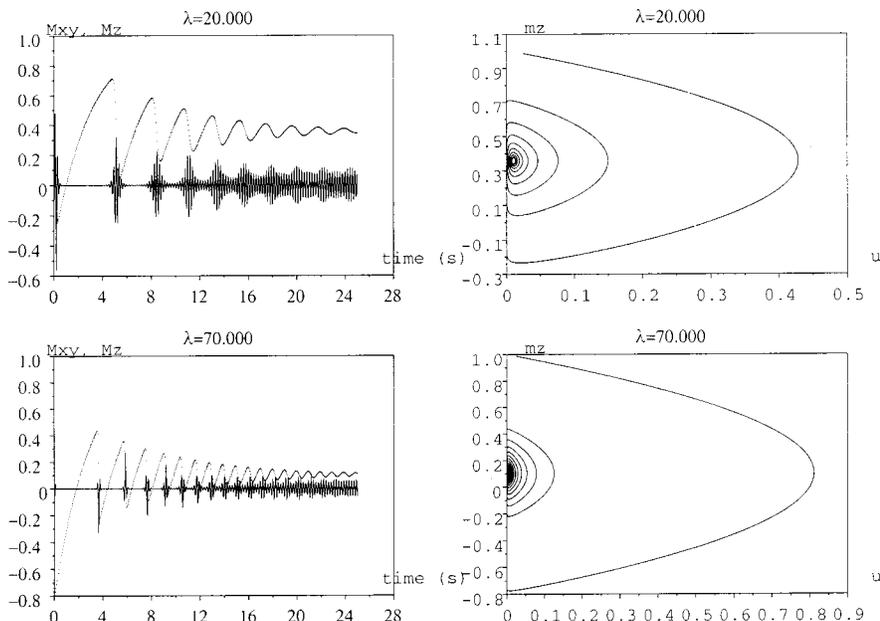
FIG. 3. (Left) Time evolution of the transverse (solid line) and longitudinal (dotted line) components of the magnetization. Note the typical bursts of longitudinal magnetization and the approach to steady-state in $1/T_1$; right: representation in the (u, m_z) space, which illustrates the focal nature of F_2. During evolution, the point (u, m_z) spirals inwards towards the focus. Trajectories are calculated for various values of λ. $T1 = 3$ s, $T_2 = 140$ ms, $\delta = -30$ Hz.

A helpful way to visualize this complicated motion is to plot the corresponding trajectory of the magnetization (see Fig. 5). One observes the repelling effect of the unstable point $F_1 = (0,1)$ for the chosen set of parameters. Due to the effect of the feedback field, the magnetization is initially driven towards the south pole, then driven back towards equilibrium by relaxation, with growing z component of the magnetization. When M_z reaches a value such that $T_{FB} > T_2$, the magnetization is repelled again and rotated back towards the south pole. The same process continues in such a way that the magnetization eventually reaches a periodic orbit, which is the three-dimensional counterpart of F_2 being an attractor for (u, m_z). Again, an important observation is that the characteristic time scale of the dynamics is very long since, according the results of previous sections, a steady state can be reached in a time which is on the order of $5T_1$.

Therefore in actual experiments, one could expect self-sustained maserlike FIDs to last for several tens of seconds.

V. EXPERIMENTAL RESULTS AND DISCUSSION

On the basis of the predictions given by the simple NLBE model, we performed experiments on a 600 MHz BRUKER DRX spectrometer using the dedicated Radiation Damping Control Unit (RDCU) hardware based on the authors' prototype[5] on a sample of 90% H_2O–10% D_2O. The basic experiment consisted in a simple acquisition following a hard pulse of a small flip angle to create in-plane magnetization. Feedback was then turned on and acquisition started. Detection of very long transients (32 s) were performed and the phase of the feedback field was varied from experiment to experiment in a systematic way from 0 to 2π
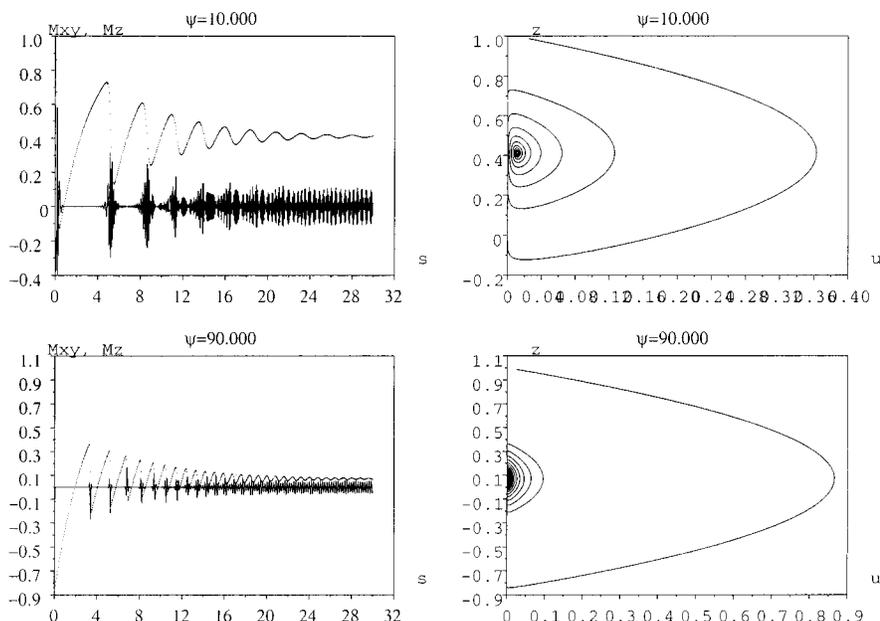

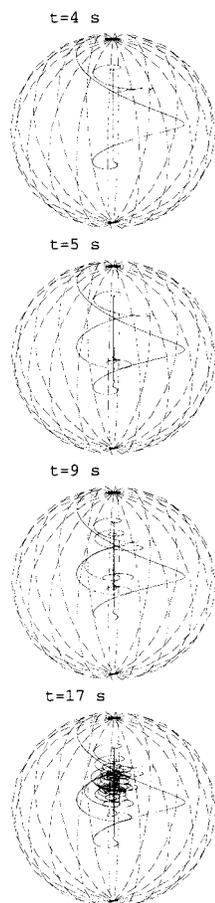FIG. 4. Same as Fig. 3 for different values of ψ.

FIG. 5. Plots of the magnetization trajectory as predicted by the NLBE model. The magnetization is initially rotated from its initial position (triangle) towards the south pole of the Bloch sphere (the position of the magnetization at the times indicated in the figure is represented by an open circle). T_1 relaxation then causes recovery of the longitudinal component, until the condition $T_{FB} < T_2$ is fulfilled. At this stage, the rotation is flipped down again towards $-z$. This process repeats until the magnetization reaches a steady state precession. Note that when ψ approaches $\pi/2$, the feedback is more efficient and the delay between successive pulses is shorter.
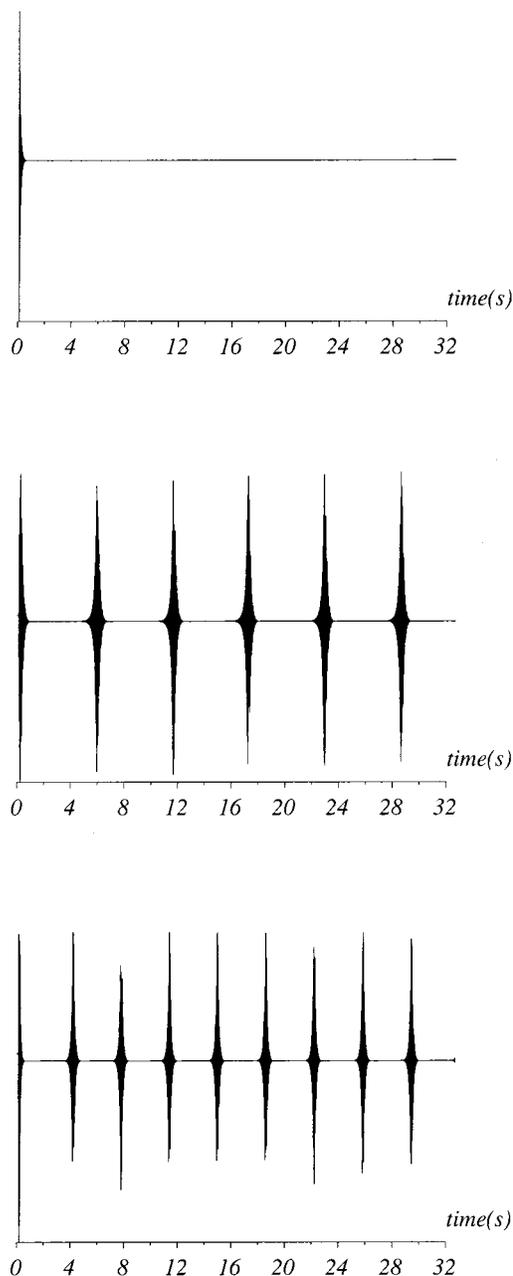

FIG. 6. Experimental observation of self-sustained maser pulses. The feedback gain used was twice the one needed for cancellation of radiation damping. The phases used in the experiments displayed correspond approximately to the following values of ψ: 50°, 30°, and −10° from bottom to top, respectively.

rad in order to observe qualitative changes of behavior of the water magnetization. Examples of induction signal are shown in Fig. 6. Typical self-sustained maser pulses were observed for a certain range of (positive) values of the feedback phase. The frequency of these bursts augmented as the feedback phase got closer to $\pi/2$, and progressively disappeared when the feedback phase approached both 0 and π. These observations thus confirmed the predictions of the NLBE model that maser pulses could be reactivated, in the presence of T_1 relaxation. It is also apparent that the time delay between consecutive maser pulses is on the order of seconds and diminishes when ψ, the phase of the applied feedback approaches $\pi/2$. This observation is consistent with the interpretation given above that a maser pulse takes place when the components of the magnetization have reached a value such that $T_{FB} < T_2$ and thus provides further experimental evidence for the role played by T_1 relaxation in this process.

However, the characteristic T_1 decay of the maser pulses amplitude could not be observed. Rather, after an initial drop

of signal intensity, the amplitudes of the FID pulses remained constant, except for small variations of their maxima, but with no attenuation with time, over a period of 32 s. It thus turned out that, although the simple model above could predict the existence of self-sustained maser pulses, it could not account for all the observed features of the detected signal. It is clear from these observations that the agreement with the NLBE based theory developed above is only qualitative.

In order to explain these discrepancies, we theoretically investigated the influence of inhomogeneous broadening of the spectral line. The Bloch equations were thus modified to incorporate the contributions of spins with different resonance frequencies. The magnetization component with fre-
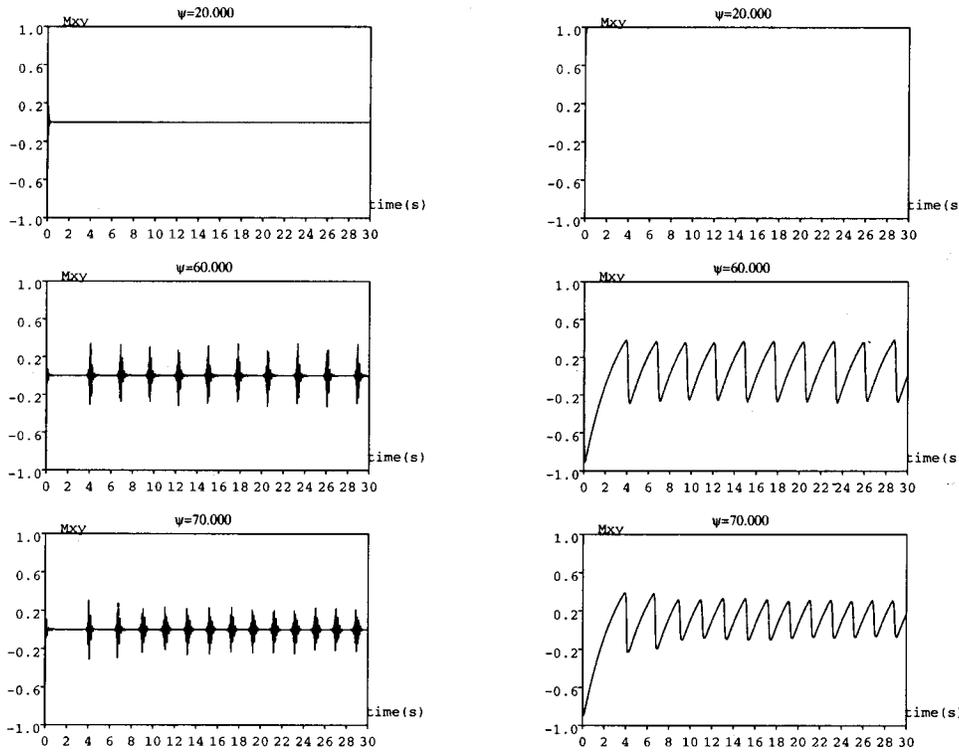
FIG. 7. Evolution of the transverse (left) and longitudinal (right) components of the magnetization in the presence of inhomogeneous broadening. The FID is a steady state of self-sustained maser pulses. Note the absence of attenuation of the maxima of the in-plane signals. See text for details.

quency $\delta\omega$, $\delta\mathbf{m}(\delta\omega)$, undergoes the action of the sum of the individual feedback fields generated by the spins from other isochromats. The frequency spreading due to inhomogeneous broadening is assumed to be described by the following Lorentzian shape function:

$$h(\delta\omega) = \frac{T_2^\dagger}{\pi} \frac{1}{1 + (\delta\omega T_2^\dagger)^2}. \tag{29}$$

Assuming that all the $\mathbf{m}(\delta\omega)$ are coupled to the probe with the same λ and ψ, one may write

$$\frac{d\mathbf{m}(\delta\omega)}{dt} = \gamma \mathbf{m}(\delta\omega) \wedge (\mathbf{B}_0 + \mathbf{B}_{FB})$$
$$- \frac{m_x(\delta\omega)\mathbf{i} + m_y(\delta\omega)\mathbf{j}}{T_2}$$
$$- \frac{(m_z(\delta\omega) - m_0(\delta\omega))\mathbf{k}}{T_1}, \tag{30}$$

where

$$\mathbf{B}_{FB} = \lambda \begin{pmatrix} \sin\psi \int_\infty^\infty m_y(\delta\omega)d(\delta\omega) + \cos\psi \int_\infty^\infty m_x(\delta\omega)d(\delta\omega) \\ -\sin\psi \int_{-\infty}^\infty m_x(\delta\omega)d(\delta\omega) + \cos\psi \int_\infty^\infty m_x(\delta\omega)d(\delta\omega) \\ 0 \end{pmatrix}. \tag{31}$$

After discretization, numerical evaluation of Eq. (30) was performed using $T_1 = 3.3$ s and $T_2 = 2.5$ s as relaxation parameters. In the calculations, the Lorentzian inhomogeneous shape function was sampled by 200 points and truncated at $\pm 2/T_2^\dagger$ with $T_2^\dagger = 140$ ms. The intensity of the feedback field was equal to twice the radiation damping field corresponding to a time constant of $T_{RD} = 10$ ms for a magnetization at equilibrium. The results of these simulations yielded FID profiles which are in very good qualitative agreement with experimental observation, as shown in Fig. 7. The particular

feature exhibited by these simulations, in addition to the existence of in-plane magnetization revivals, is the absence of damping of the maxima of these maser bursts. This suggests the existence of a steady state of maser pulses in which the magnetization generates an rf field leading to its (partial) own inversion. During the period following a burst, T_1 relaxation is the predominant dynamical process and allows for the recovery of the magnetization which in turn leads to the generation of the next rf (maser) pulse and inversion of the magnetization. These simulations very closely reproduce ex-

perimental observations (see Fig. 6). Further numerical computations (not shown) confirm that when inhomogeneous broadening is reduced (larger values of $T_2^\dagger$), damping of the magnitude of the maser pulses is observed, and as $T_2^\dagger$ is increased the calculated induction signal tends to one obtained with the simple NLBE model in which no static field inhomogeneity is assumed.

Confronting these results with the NLBE model, it is possible to explain the absence of damping of these self-sustained maser pulses and the onset of what happens to be a steady state of maser oscillations. Indeed, considering again the case where $\mathbf{B}_0$ inhomogeneity is not taken into account, it is seen (see for instance Fig. 4) that successive maser pulses are triggered for smaller longitudinal magnetization and larger transverse magnetization. This is associated with a progressively reduced efficiency of the feedback (longer T_{FB}) and a shorter time interval between the pulses. Alternatively, a slightly different picture can be given for the situation where inhomogeneous broadening is present. In that case, once the magnetization has been inverted and the feedback field has become too weak to maintain collective motion of the spins, the isochromats get dephased, leading to almost complete loss of net transverse magnetization, and essentially relax towards equilibrium through T_1 and T_2 processes. Then after a certain period of time, some of the isochromats have recovered a total magnetization which is high enough to induce phase coherence again with spins having different precession frequencies. This causes the reappearance of collective motion of the spins and the next maser pulse occurs. However, in contrast to the NLBE model, when sufficiently large frequency dispersion exists, $\mathbf{B}_0$ inhomogeneities seem to prevent systematic buildup of transverse magnetization from pulse to pulse, thus allowing for the setup of a steady state of self-sustained maser pulses without progressive decay of the in-plane signal which would eventually lead to their disappearance. Finally, it should be remarked that the phenomenon described in this paper should be clearly distinguished from multiple spin echoes induced by radiation damping reported in Ref. 15 and 16. Indeed, in the experiments presented here, the revivals of the in-plane magnetization are not caused by refocusing of the magnetization and, as shown above, the basic mechanism involved is completely different by nature. Indeed, in contrast with the multiple echo phenomenon, each isochromat generates its own feedback field and at the same time undergo the action of the feedback fields generated by all other isochromats in the sample. When, after a pulse, an isochromat "feels" a strong enough feedback field, the motion of its magnetization is dominated by a rotation about this magnetization-dependent field. A feedback field which grows in intensity is therefore able to progressively induce collective motion of the magnetizations originating from other isochromats and phase coherence between them. Because of the presence of inhomogeneous broadening, this phase coherence is lost after each pulse and the sequence of events goes on again. It should be stressed again that, as discussed above, periodic revival of collective motion of the spins originates from the interplay between a T_1 relaxation process and a back action of the probe onto the magnetization. In this respect, inhomogeneous broadening has the function of a superimposed phenomenon which alters only qualitatively the predictions of the simpler NLBE model.

VI. CONCLUSION

In this paper, we have investigated both theoretically and experimentally the unconventional behavior of a large magnetization subject to a feedback field from the detection circuit of the probe. A simple model (NLBE) allowed us to predict the occurrence of repeated maser pulses during the course of evolution. These were explicitly related to the existence of T_1 relaxation in the evolution equations and to the combination of both this T_1 process and feedback from the probe. Moreover, in contrast with the predictions of this simple model, a characteristic attenuation of the maser amplitude could not be observed experimentally. This was interpreted by taking into account line broadening caused by an inhomogeneous static magnetic field. Further investigations are underway to better characterize the complexity of this intriguing phenomenon.

[1] N. Bloembergen and R. V. Pound, Phys. Rev. **95**, 8 (1954).
[2] A. Abragam, *The Principles of Nuclear Magnetism* (Clarendon, Oxford, 1961).
[3] V. J. Sklenar, J. Magn. Reson. **114**, 132 (1995).
[4] P. Broakaert and J. Jeener, J. Magn. Reson. **113**, 60 (1995).
[5] A. Louis-Joseph, D. Abergel, and J.-Y. Lallemand, J. Biomol. NMR **5**, 212 (1995).
[6] C. Anklin, M. Rindlisbacher, G. Otting, and F. H. Laukien, J. Magn. Reson. **106**, 199 (1995).
[7] D. Abergel, A. Louis-Joseph, and J.-Y. Lallemand, Chem. Phys. Lett. **262**, 465 (1996).
[8] D. Abergel, A. Louis-Joseph, and J.-Y. Lallemand, J. Chem. Phys. **112**, 6365 (2000).
[9] S. Bloom, J. Appl. Phys. **28**, 800 (1957).
[10] R. Hobson and R. Kayser, J. Magn. Reson. **20**, 458 (1975).
[11] T. Barbara, J. Magn. Reson. **98**, 608 (1992).
[12] J. A. Guckenheimer and P. Holmes, *Nonlinear Oscillations, Dynamical Systems, and Bifurcations of Vector Fields* (Springer, New York, 1983).
[13] D. K. Arrowsmith and M. Place, *Differential Systems: Differential Equations, Maps, and Chaotic Behavior* (Chapman and Hall, New York, 1992).
[14] This effect was in fact anticipated some time ago; see J. Jeener, P. Broakaert, and A. Vlassenbroek, Collective effects in high resolution liquid NMR, *Lecture Notes for the 14th Waterloo NMR Summer School, June 16–21, 1997*.
[15] J. Jeener, A. Vlassenbroek, and P. Broakaert, J. Chem. Phys. **103**, 1309 (1995).
[16] M. P. Augustine and E. L. Hahn, J. Chem. Phys. **107**, 3324 (1997).